Dynamic Imaging on the High Resolution Research Tomograph(HRRT): Non-Human Primate Studies

Vesna Sossi, *Member IEEE,* Marie-Laure Camborde, Stephan Blinder, A Rahmim, *Member IEEE*, Kevin J-C Cheng, Ken R Buckley, Doris J Doudet, Thomas J Ruth

***Abstract*–The high resolution research tomography (HRRT) is currently the most complex human brain scanner due to its ability to detect the gamma depth of interaction, its octagonal geometry, and the large number of crystals (119,808) leading to approximately 4.5 x 10^9 possible lines of response (LORs). Reconstruction of dynamic studies on this scanner is particularly challenging due to the dynamic range of both, number of acquired events per frame and acquisition count rates. Some artifacts have been observed with phantom studies: here we evaluate their impact on time activity curves (TACs) and binding potential (BP) values in realistic scanning situations with the ultimate goal of defining an efficient and accurate image reconstruction protocol. Non-human primate studies were used for this purpose. We compared TACs and BPs obtained from images reconstructed with three different reconstruction algorithms, two different axial spanning configurations and detector normalization factors obtained from two different data sets. We also compared BP values obtained from scans of the same animal performed on the Siemens ECAT 963B and the HRRT under identical conditions. The statistical reconstruction methods produced nearly identical results and the impact of emission/normalization count rate mismatch was found to be effectively negligible. Likewise no image degradation due to increased axial spanning was observed. Data obtained from the analytical method were less robust and in general much more sensitive to noise, thus demonstrating a suboptimal performance of this algorithm. The BP values obtained with the HRRT were by approximately 50% higher compared to those obtained in the ECAT as a result of the increased resolution of this tomograph.**

I. Introduction

THE high resolution research tomography (HRRT) is currently the most complex human brain scanner due to its large number of crystals (119,808) and ability to decode the depth of γ interaction in the crystal. The crystals are grouped into 8 detector heads, leading to an octagonal design with gaps in between heads. The number of possible lines of response (LORs) is approximately 4.5 x 10^9, which is the highest number of possible LORs in any human scanner leading to associated challenges in data processing and reconstruction. The use of analytical reconstruction algorithms, which are known to preserve linearity with the imaged concentration, tends to lead to artifacts due to the necessary gap filling step and to a relatively poor noise control. Statistical reconstruction algorithms on the other hand, while better able to account for the presence of gaps, tend to be very CPU intensive and prone to inaccuracies in a situation where only a low number of counts is acquired in any specific time frame. Such inaccuracies are highly dependent on the specific algorithm and details of its implementation (1).

Dynamic studies on the HRRT (2, 3) provide very stringent testing grounds for efficient and accurate data quantification and reconstruction, due to the large dynamic range of both, the number of acquired events per frame and acquisition count rates. The accuracy of several reconstruction algorithms and detector normalization procedures has already been tested with high statistics phantom studies and artifacts and differences have been observed (1, 4, 5). However not much is known about the impact of such differences on images acquired under realistic scanning situations, where the uncertainties due to the often count limited data sets might dominate over systematic errors. The goal of this study was to evaluate the impact of such artifacts on data obtained in representative realistic scanning situations. We used two non-human primate studies, performed at different count-rates and compared both, time activity curves for selected regions and related binding potentials as a function of (i) emission/normalization count rate mismatch, (ii) reconstruction algorithm, (iii) axial spanning (degree of axial binning). Three reconstruction methods were evaluated: FORE + DIFT (Fourier rebinning – direct inverse Fourier transform), 3DOP (3D - Ordered subset expectation maximization - Ordinary Poisson) (6) and a newly developed list mode based Ordinary Poisson reconstruction method (LM-OP) (7-8). In addition, we also compared time activity curves (TACs) and binding potential (BP) estimates obtained on the HRRT to those obtained in a previous generation scanner, the Siemens ECAT 953B (9) to evaluate the impact of the higher scanner resolution on the biological measures.

II. Methods

A. Scans

Subject 1. A non-human primate underwent a 60 min ^{11}C-dihydrotetrabenazine (DTBZ – a vesicular monoamine transporter VMAT2 marker) scan on the HRRT (after a 6 min transmission scan and a 5mCi bolus injection). Data were

V.S. is with the University of British Columbia, Vancouver, B.C., Canada, V6T 1Z1 (telephone 604 822 7710, e-mail vesna@phsyics.ubc.ca)

M-L. C. is with TRIUMF, Vancouver B.C., Canada V6T 2A3 (e-mail marie@pet.ubc.ca)

S.B. is with TRIUMF, Vancouver B.C., Canada V6T 2A3 (e-mail blinder@phas.ubc.ca)

A.R. was with the University of British Columbia, Vancouver, B.C., Canada V6T 1Z1. He is now with the Dept. of Radiology, Johns Hopkins University School of Medicine, Baltimore, MD 21205 (e-mail arahmim1@jhmi.edu).

K.C. is with the University of British Columbia, Vancouver, B.C., Canada V6T 1Z1 (e-mail jcheng@physics.ubc.ca)

D.D. is with the University of British Columbia, Vancouver, B.C, Canada V6T 2B5 (e-mail ddoudet@interchange.ubc.ca) CHECK POSTAL CODE

T.J.R. is with TRIUMF, Vancouver B.C., Canada V6T 2A3 (e-mail truth@triumf.ca)

acquired in list mode and then framed into a 5x1min, 5x5 min and 4x7.5 min framing sequence. The number of counts/frame in this study ranged from 13M to 140M (see figure 1) and the count rate ranged between 600 and 50 kcps. 120 min later the same animal was scanned on the ECAT 953B with an identical scanning protocol.

Subject2. A non-human primate was injected (bolus + constant infusion) with a total of 5mCi of the dopamine D2 receptor antagonist ^{11}C-raclopride (RAC) and scanned for 60 min after performing a 6 min attenuation scan with a ^{137}Cs source. The same framing sequence was used for this study. The number of counts/frame ranged from 8M to 42M (figure 1), while the count rate ranged between 200 and 25 kcps. This animal was scanned only on the HRRT.

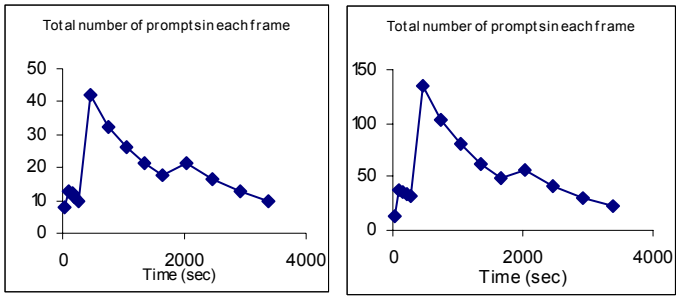

Figure 1. Total number of events for the two studies - study 1 right and study 2 left.

B. Data processing

HRRT-Detector normalization factors. Two different sets of normalization factors were used, one calculated from data acquired at ~ 610 kcps (NORM1) and the other calculated from data acquired at ~ 120 kcps (NORM2).

HRRT-Reconstruction methods. For each normalization data set three reconstruction methods were used: FD, 3DOP with 16 angular subsets and 6 iterations, followed by a 2 mm FWHM gaussian filtering and LM-OP with 16 temporal subset and 6 iterations followed by a 2 mm FWHM gaussian filtering. The two sinogram based reconstruction methods, FD and 3DOP, were applied to data binned in axial span 3 (individual sinograms binned into a 1-2-1 pattern) and axial span 9 (individual sinograms binned into a 4-5-4 pattern). The reconstruction time for data binned in span 9 is approximately 60% faster compared to that required to reconstruct data binned in span 3.

The two statistical algorithms, 3DOP and LM-OP, include the same scatter and smoothed random estimate in the image update factor (10-11). It is interesting to point out that these two algorithms are conceptually identical, with the exception of using time as opposed to angular subsets in the image update step. In this implementation of LM-OP the time subsets are formed by dividing the entire frame length into three parts. Each time subset is then formed by grouping a sixteenth part of each of the three parts. All data were corrected for dead time.

ECAT 953B. Dead time, normalization, scatter and attenuation corrected data were reconstructed using FORE + 2DFBP, following our standard processing method for ECAT 953B data acquired in 3D mode (12).

C. Data analysis

Three approximately 19.5mm^2 regions of interest (ROIs) were placed on each striatum (caudate, putamen and ventral striatum) and six approximately 41.4 mm^2 ROIs were placed on the occipital cortex. The ROIs were placed on five adjacent HRRT planes and two ECAT planes (for study 1) so as to approximately match the axial extent of the ROI (~ 6 mm). The reference region ROI and related TAC was obtained as average of the six cortical ROIs. For study 1 the placement and size of the ROIs was visually matched as close as possible between the two scanners. Data were compared in terms of TACs and BP values which were approximated by the ratio between the striatal ROI values and reference region ROI values – 1. The TAC comparison was performed by estimating the average ratio between individual TACs points obtained under the selected circumstances of interest and the minimum and maximum values of such ratio across all time points.

III. Results and Discussion

A. Effect of emission and normalization count rate mismatch.

Figures 2 and 3 show the impact of the normalization scan count rate on the BP estimate and TACs for each reconstruction algorithm for both studies. In principle, the count rate of study 2 is better matched by NORM2, while the count rate of study 1 spans the count rate of both normalization data sets. In spite of these count rate variations no systematic differences in either the BP or TAC values were found as a function of normalization count rate.

Overall, there is very little difference (< 5%) between the BP and TAC values obtained with the two normalization data sets for the statistical reconstruction algorithms for either study. The biggest variation is observed for both variables (> 10% for BP and 25% for the TAC comparison) for FD span 3, particularly for study 2, which had less counts, indicating the poor performance and sensitivity to noise exhibited by of this algorithm.

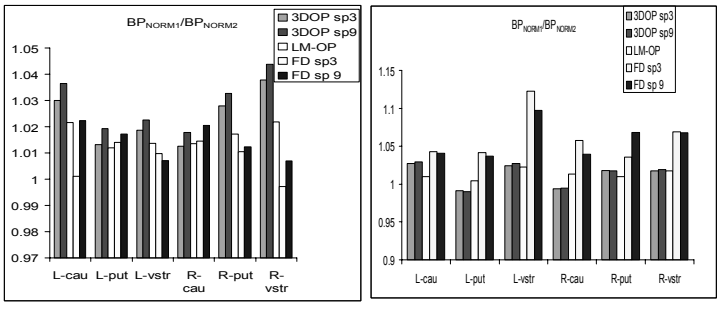

Figure 2. Ratio of BP values obtained with each NORM for each region and each reconstruction method. Study 1 on the left, study 2 on the right.

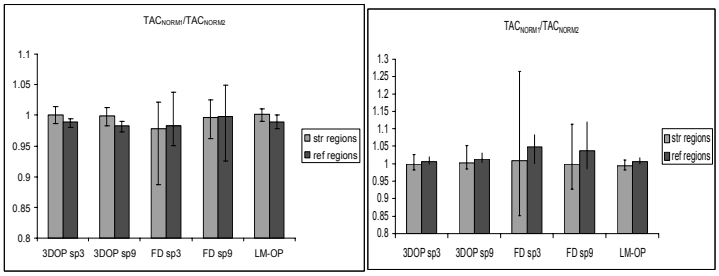

Figure 3. Average ratio of TAC points and ratio minimum and maximum ratio value. Results are averaged over striatal and background regions separately. Study 1 on the left, study 2 on the right.

B. *Effect of axial span*

Figures 4 and 5 show the effect of span on the BP estimate and comparison of TAC points for 3DOP and FD for both studies. For 3DOP, data obtained from span 9 and span 3 are virtually identical for both studies regardless of normalization, both when comparing the BP and individual TAC points values (agreement within ~ 1%). In contrast, a bigger variability is observed when comparing the TAC points obtained with FD, even though the mean values for the variables are very close.

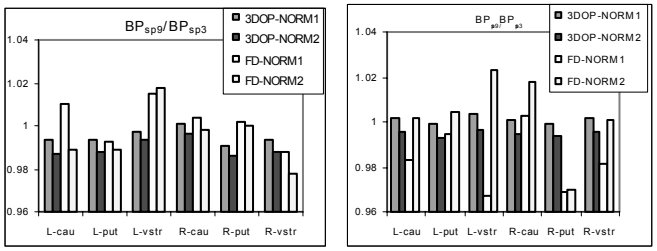

Figure 4. For each reconstruction method BP values obtained with span9 normalized to those obtained with span3. Study 1 on the left, study 2 on the right.

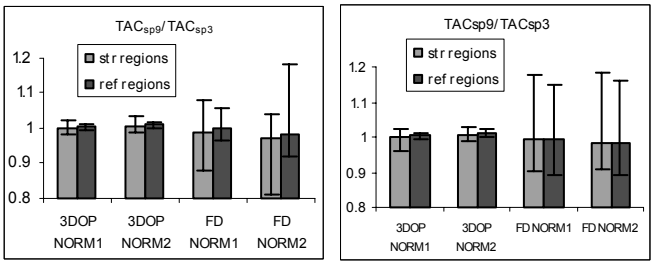

Figure 5. Average ratio of TAC points and ratio minimum and maximum ratio value. Results are averaged over striatal and background regions separately. Study 1 on the left, study 2 on the right. Data are averaged separately over the striatal and the reference regions.

C. *Effect of reconstruction algorithm*

Figure 6 shows the BP obtained with LM-OP and FD (span3) normalized to BP obtained with 3DOP (span3) using NORM1. Almost identical results were obtained for NORM2. The statistical reconstruction algorithms provide very similar results (within ~ 5%): the BP values are closer for study 1, which had a higher number of counts/frame. The agreement with FD is less good and more variable.

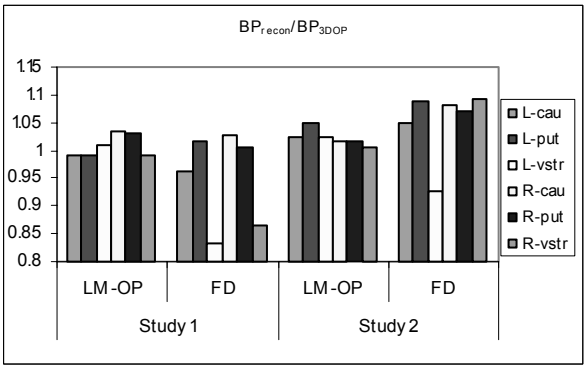

Figure 6. BP obtained with the algorithms described in the x-axis normalized to BP obtained with 3DOP for the six striatal regions described in the legend (see methods).

D. *Specific comparison of LM-OP and 3DOP.*

Although conceptually identical, 3DOP and LM-OP still showed some minor variations in tracer concentration estimates especially when a relatively low number of counts/frame was acquired and a systematic difference in the first frame for all ROIs (figure 7).

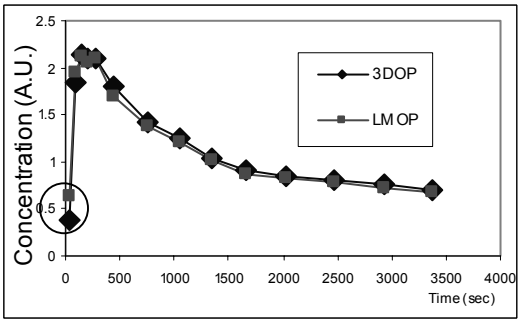

Figure 7. Sample TACs. Note the concentration overestimation by LM-OP in the first frame – encircled.

The reason for the systematic difference was traced to the nature of the time subsets coupled with a very fast increase in the number of counts during the first minute after tracer injection (figure 8). The later time subsets contain a higher than average number of counts compared to the earlier time subsets in spite of some degree of time interleaving. Since, the later time subsets are used in the final image update steps, they introduce an upwards bias in the estimated radioactivity level. When list mode data were reconstructed using one subset only the agreement between LM-OP was restored (figure 8).

Random variations were attributed to the fact that although the two methods use the same overall data, the subsets are not identical: in a situation of low counts, statistical differences in the subsets may lead to a different final image.

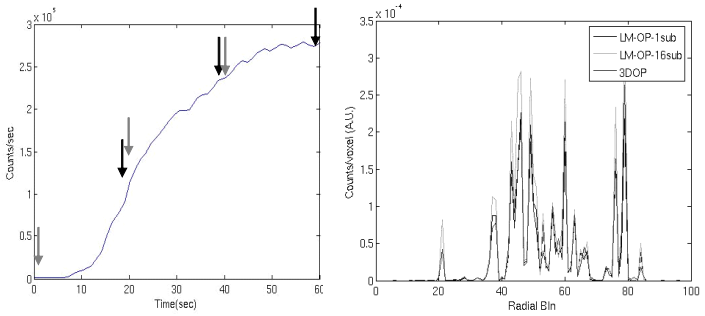

Figure 8. Left - count rate variation during the first frame of study 2. Grey arrows indicate the approximate time-regions of the data contributing to the first subset, while the black arrows indicate the time-regions of the data contributing to the 16th subset. Right - profiles through a single image of the first frame of study 2 (~ 7M counts). LM-OP performed with one subsets agrees much better with 3DOP while a clear overestimation is observed for data reconstructed with LM-OP 16 subsets.

Such difference tends to disappear as the number of acquired events increases. This is illustrated in figure 9 where the same profiles through single slices are shown for two adjacent time frames of study 1: frame 4 with approximately 30M counts and frame 5 containing approximately 130 M counts. A much better agreement between the profiles is observed for the image obtained from data sets containing more counts.

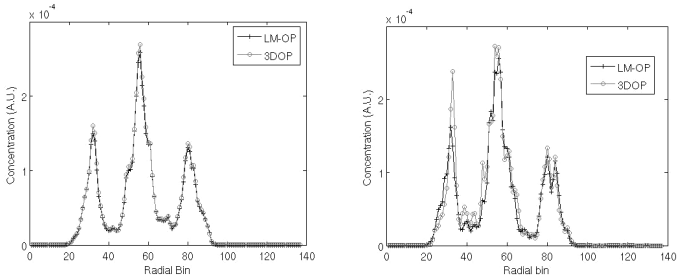

Figure 9. Profiles through the same slice. Profiles obtained from images reconstructed from a data set containing 30M counts - right, profiles obtained from images reconstructed from a data set containing 130M counts - left.

E. Comparison to the data obtained on the ECAT 953B

Figure 10 shows a representative image obtained on the HRRT compared to an equivalent image obtained on the ECAT 953B. The comparison between the BP values obtained from identical scanning protocols of the same animal on the two scanners is illustrated in figure 11. In average the BP values obtained on the HRRT are approximately 50% higher compared to those measured on the ECAT 953B, fairly uniformly over the target regions. Some degree of region dependency in the results of the comparison is to be expected, since the ROI placement on the two image data sets, although optimally matched, was still not identical. Furthermore the anatomical size of the striatal regions was not identical thus leading to a somewhat variable impact of the partial volume effect.

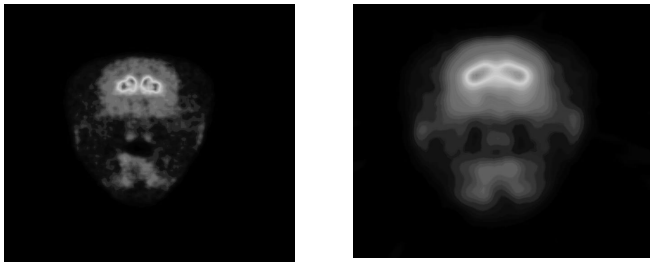

Figure 10. HRRT image - left (HRRT resolution ~ $(2.5\text{mm})^3$); ECAT image – right (ECAT resolution ~ $(6\text{ mm})^3$). In both cases the axial slice thickness was adjusted to approximately 6 mm by summing the appropriate number of individual slices.

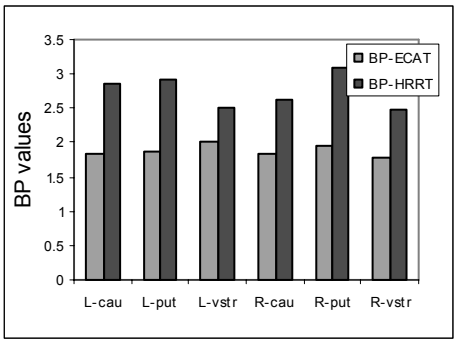

Figure 11. Comparison of BP values obtained with the HRRT and the ECAT 953B for six striatal regions. Data were obtained for the same subject scanned under identical conditions on the two scanners.

Data from the HRRT and the ECAT 953B were also compared on a TAC level (figure 12).

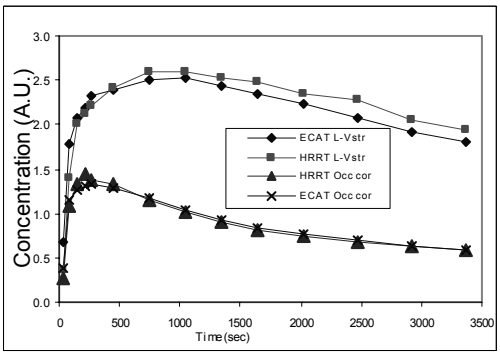

Figure 12. Comparison of sample TAC between the HRRT (3DOP sp 3) and ECAT for the ventral striatum and the occipital cortex. Curves are normalized by their mean.

The overall shape of the reference region TAC was found to be very similar between the two scanners which supports the fact that the HRRT provides accurate dynamic information; the reference region is not expected to suffer from partial volume effect on either scanner, therefore the shapes of the two reference region TACs are expected to be extremely similar, if the data are reconstructed correctly. The difference in the shape of the striatal TAC is to be attributed to a different amount of partial volume effect on the two scanners.

IV. Conclusions

This study addresses the feasibility and accuracy of dynamic imaging in a high resolution brain scanner with depth of interaction capabilities. It was found that in a realistic scanning situation the impact of instrumentation related systematic artifacts due to the mismatch between the normalization and emission count rate was nearly negligible.

Three reconstruction algorithms were investigated. Of the three, one of them (FD) was based on an analytical approach and was found to be less robust and more susceptible to noise compared to the other two, 3DOP and LM-OP and should thus not be used. A detailed comparison of 3DOP and LM-OP showed that these two algorithms produce very similar results and are equally insensitive to emission/normalization count rate mismatch. However, while the agreement between the two reconstruction methods is excellent in a situation where a large number of events/frame is acquired, there are observable statistical variations in a situation where a lower number of events/frame are present (< ~ 50M). Furthermore it was found that in a situation of rapidly changing number of counts within a frame, the LM-OP, in its current implementation, produces biased results. A different subset selection scheme is currently under investigation and will be easily implemented.

It was demonstrated that 3DOP applied to data binned in span 9 produces identical results to those obtained from data reconstructed using span 3 sinograms, while reducing reconstruction times by approximately 60%. It is thus apparent that LM-OP (with a new subset selection scheme) and 3DOP with data rebinned in span 9 both provide robust and efficient reconstruction methods suitable for the reconstruction of dynamic data on the HRRT. The choice between the two will depend on the number of acquired data in each frame – a direct comparison between the computation times required by each is at present beyond the scope of this study, since the two codes did not undergo the same level of computational optimization.

Finally, a comparison of BP values obtained with the HRRT to those obtained with an ECAT 953B showed an approximately 50% increase in BP values, while still maintaining the same shape of the reference region time activity curve. This increase was attributed to the higher resolution achieved by the HRRT and shows great promise for the feasibility of new biological investigation that will be made possible by this scanner.

Acknowledgment

The authors would like to thank the UBC/TRIUMF PET team for assistance with scanning, Ziad Burbar, Dr. Christian Michel and Dr. Merence Sibomana from Siemens Medical Solutions for useful discussions. This work was supported by a Natural Sciences and Engineering Research Council of Canada, a Michael Smith Foundation for Health Research, a Canadian Institutes for Health Research and a TRIUMF Life Sciences grant.

References

[1] A. Rahmim, M. Lenox, A. J. Reader, C. Michel. Z. Burbar, T. J. Ruth, and V. Sossi, "Statistical list-mode image reconstruction for the high resolution research tomography," *Phys. Med. Biol.*, vol. 49, pp. 4239-4258, 2004

[2] K. Wienhard, M. Shmand, M. E. Casey, K. Baker, J. Bao, L. Eriksson, W. F. Jones, C. Knoess, M. Lenox, M. Lercher, P. Luk, C. Michel, J. H. Reed, N. Richerzhagen, J. Treffert, S. Vollmar, J. W. Young, W. D. Heiss, and R. Nutt, "The ECAT HRRT: Performance and First Clinical Application of the New High Resolution Research Tomograph," *IEEE Trans. Nucl. Sci.* vol. 49, pp. 104-110, 2002

[3] V. Sossi, H. W. A. M. de Jong, W. C. Barker, P. Bloomfield, Z. Burbar, M.-L. Camborde, R. E. Carson, C. Comtat, L. A. Eriksson, S. Houle, D. Keator, K. Christof, R. Krais, A. A. Lammertsma, A. Rahmim, M. Sibomana, M. Teräs, C. J. Thompson, R. Trébossen, J. Votaw, K. Wienhard, D Wong,The Second Generation HRRT - a Multi Centre Scanner Performance Investigation, Proceedings of the 2005 IEEE/MIC

[4] Boellaard R, Lubberink M, de Jong H, Kropholler M, Lammertsma AA, Application of various iterative reconstruction methods for quantititatve 3D dynamic brain PET studies, Proceedings of the IEEE/MIC 2004

[5] S. Blinder, M.-L. Camborde, K. R. Buckley, A. Rahmim, J.-C. Cheng, T. J. Ruth, V. Sossi, Influence of Depth of Interaction on Spatial Resolution and Image Quality for the HRRT, Proceedings of the 2005 IEEE/MIC

[6] D. G. Politte and D. L. Snyder, "Corrections for Accidental Coincidences and Attenuation in Maximum-Likelihood Image Reconstruction for Positron-Emission Tomography," *IEEE Trans. Med. Imag.*, vol. 10, no. 1, pp. 82-89, 1991

[7] A. Rahmim, J.-C. Cheng, S. Blinder, M-L Camborde, and V. Sossi, "Statistical dynamic image reconstruction in state-of-the-art high resolution PET," Phys. Med. Biol., vol. 50, pp. 4887-4912, 2005

[8] J.-C. Cheng, A Rahmim, S Blinder, M.-L. Camborde, V. Sossi, Implementation of scatter corrected List-Mode OP-EM reconstruction algorithm and a dual (Histogram/List-Mode) reconstruction scheme for dynamic PET imaging, Proceedings of the 2005 IEEE/MIC

[9] Spinks TJ, Jones T, Bailey DJ, Townsend DW, Grootoonk S, Bloomfield PM, Gilardi M-C, Casey ME, Sipe B, Reed (1992) Physical performance of a positron tomograph for brain imaging with retractable septa. *Phys Med Biol* 37: 1637-1655

[10] C. C.Watson, "New, Faster, Image-Based Scatter Correction for 3D PET," *IEEE Trans. Nucl. Sci.* , vol. 47, pp. 1587-1594, 2000

[11] Byars L, Sibomana M, Burbar Z, Jones J, Barker WC, Liow J-S, Carson R, Michel C, Variance Reduction on Randoms from Delayed Coincidence Histograms for the HRRT, Proceedings of the 2005 IEEE/MIC

[12] Sossi V, Oakes TR, Chan G, Ruth TJ. Quantitative comparison of 3D and 2D PET with human brain studies. J Nucl Med 1998;39:1714-1719